

Impact of sensor ageing on iris recognition



Thomas Bergmüller^{*†}, Luca Debiasi^{*}, Zhenan Sun⁺ and Andreas Uhl^{*}

^{*}University of Salzburg, Austria

[†]Authentic Vision, Austria

⁺National Lab for Pattern Recognition CASIA, China

tb@authenticvision.com, {ldebiasi,uhl}@cosy.sbg.ac.at, znsun@nlpr.ia.ac.cn



Abstract

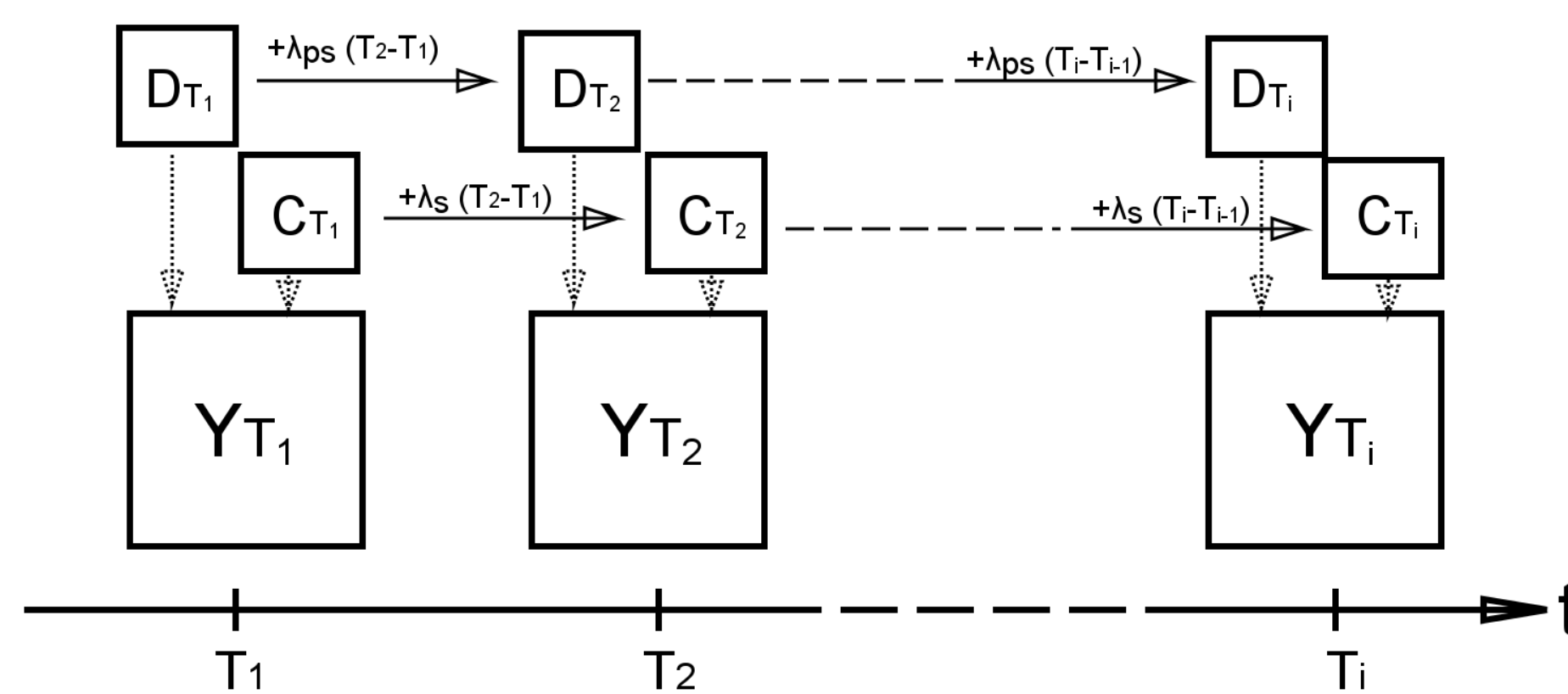
Similar to the impact of ageing on human beings, digital image sensors develop ageing effects over time. Since these imager's ageing effects (commonly denoted as pixel defects) leave marks in the captured images, it is not clear whether this affects the accuracy of iris recognition systems. This paper proposes a method to investigate the influence of sensor ageing on iris recognition by simulative ageing of an iris test database. A pixel model is introduced and an ageing algorithm is discussed to create the test database. To establish practical relevance, the simulation parameters are estimated from the observed ageing effects of a real iris scanner over the timespan of 4 years.

Introduction

Some researchers claim that iris-related information is stable or relatively stable over time, while others observe significant changes. They mostly conclude these **age-dependent changes in iris texture** by observing **changes in a system's iris-recognition rate**.

To investigate this issue, one would need to have identical data captured at at least two significantly different points in time under identical conditions. **As a human being ages, so does the sensor.** For this reason **one cannot capture test data to investigate the sensor's or the subject's ageing** in an isolated manner physically.

Generation of virtually aged data



- The defect matrices C and D are computed recursively
- **Earlier developed defects are maintained over virtual age**

Experimental setup

- Sensor: *Irisguard H100 IRT*
 - Iris texture images acquired in **2009 and 2013**
- We performed a device identification experiment (exploiting the sensor's PRNU) to ensure that the **same sensor was used at both dates**.

Results

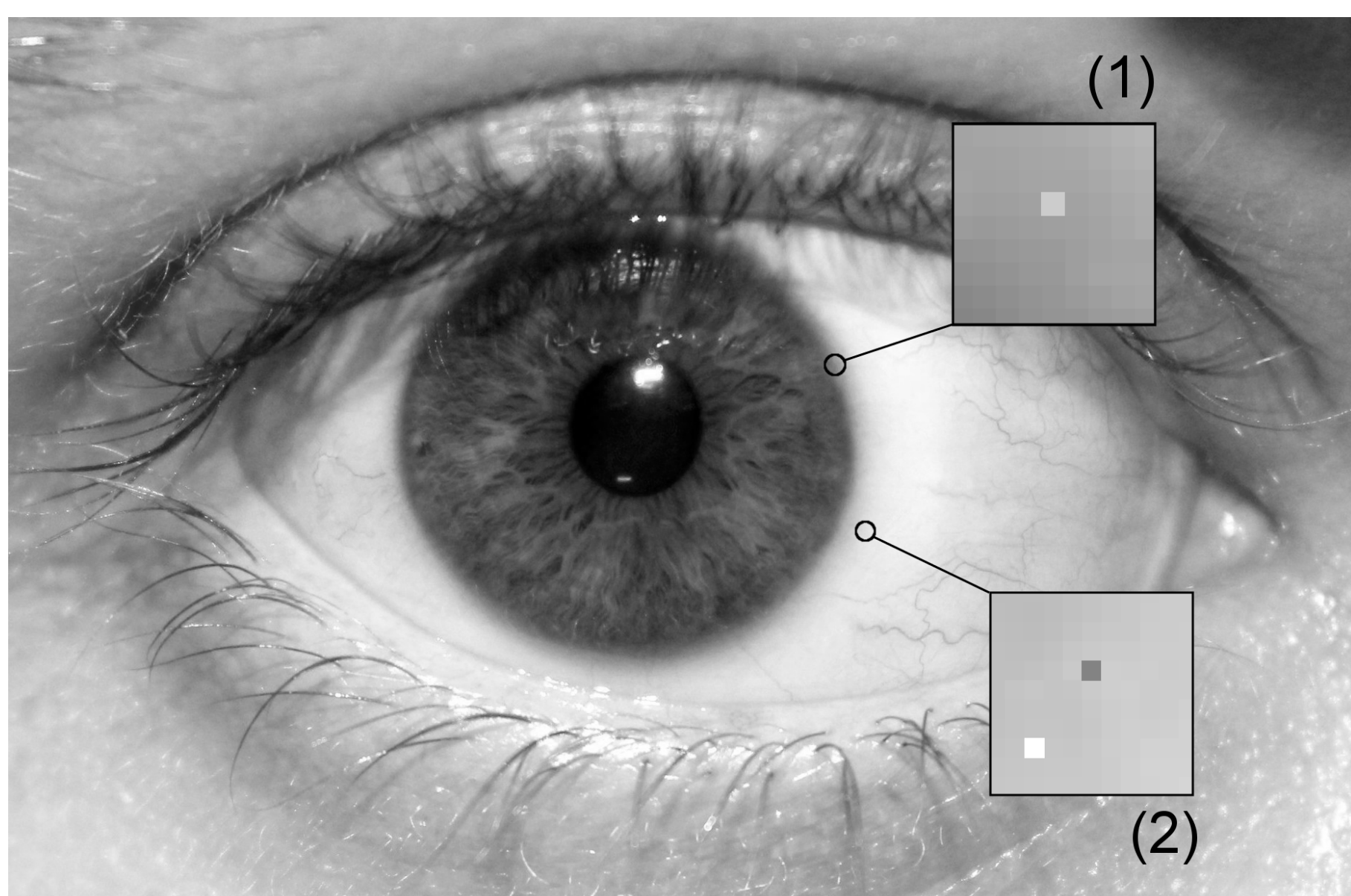
Tested algorithms with generated aged data sets (based on IITD data base):

- Rathgeb and Uhl (cb and cr)
- Ko *et al.* (ko)
- Monroe *et al.* (dct)
- Ma *et al.* (qsw)
- LogGabor-1D method by Masek (lg)

Sensor Ageing and Pixel Model

Defect types that develop over time as the sensor ages are:

- **Stuck pixels**: pixel with constant offset
- **Hot pixels**: extremely high dark current
- **If a pixel is once defective, it remains defective**



A *partially-stuck or hot pixel* (1) and two *stuck pixels* (2) in an iris image (enhanced for visualisation).

After omitting negligible factors the pixel output model is defined as

$$Y(x, y) = \begin{cases} C(x, y) & \text{if } C(x, y) \neq 0; \\ I(x, y) + D(x, y) & \text{otherwise.} \end{cases}$$

with $Y, C, I, D \in (\mathbb{Z} : [0; 255])^{w \times h}$

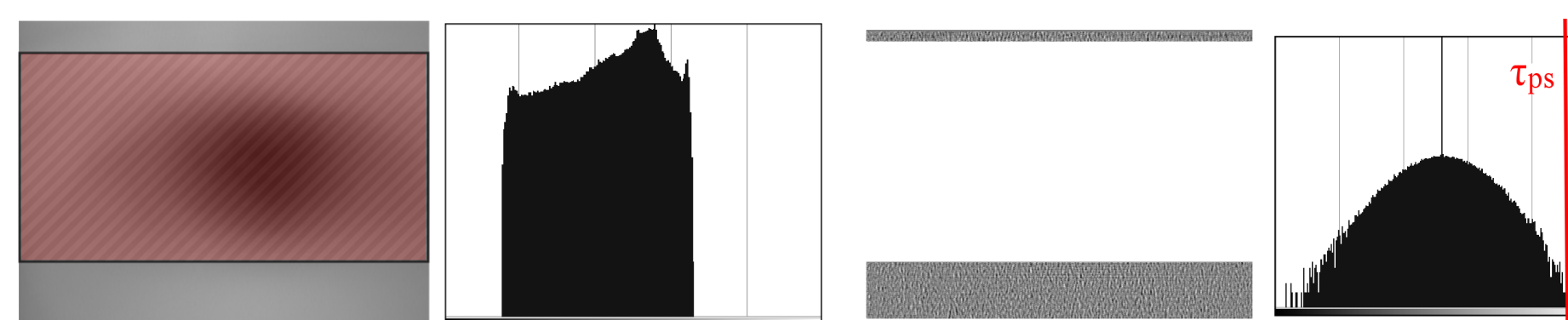
where Y is the resulting pixel output, I the incident light, C stuck and D partially-stuck pixels.

Parameter estimation from iris database

Defect growth rates and amplitudes are retrieved from a data base captured with a real iris scanner. Because the image centre contains correlated data, the parameters are estimated from uncorrelated regions, i.e. regions showing skin.

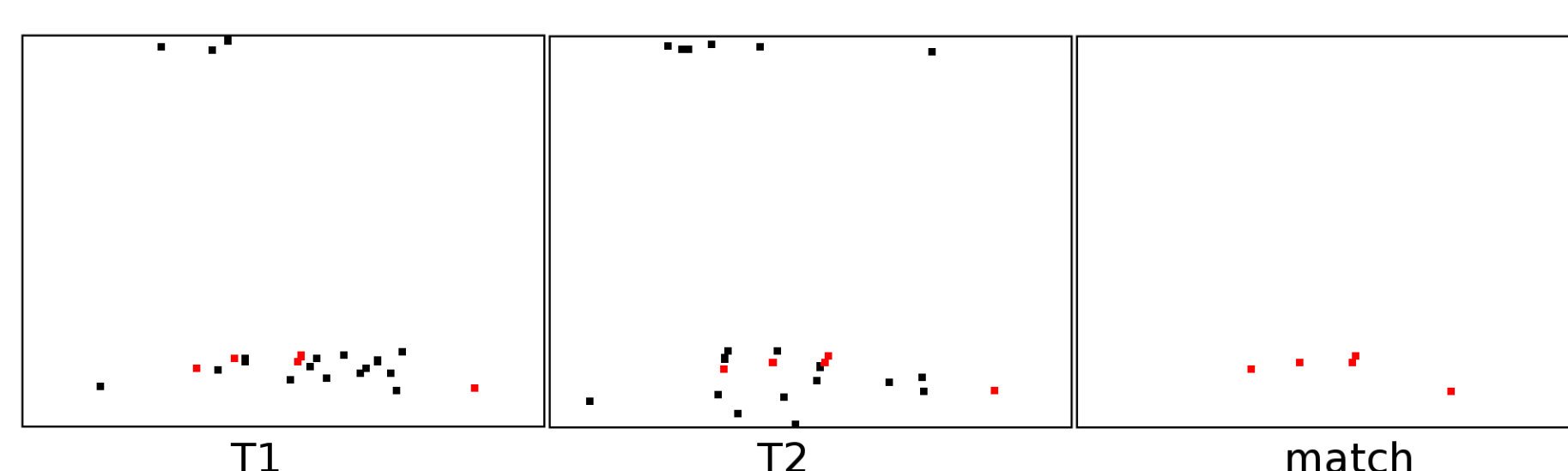
- **Stuck pixels** \rightarrow constant pixel value in multiple images
- **Hot pixel** \rightarrow offset between median-filtered and original mean grey image

The offset image's logarithmic histogram shows normal distribution due to PRNU. The **decision threshold τ_{ps}** is chosen in a way that **only outliers are declared as partially-stuck pixels**.



From left to right: mean grey image (correlated region marked), histogram of grey values in uncorrelated regions, pixel offsets, logarithmic histogram of pixel offsets with decision threshold τ_{ps} .

Correctly classified pixel defects from T_1 are contained in T_2 as well. All other detected defects in T_1 can be interpreted as misclassification, since they violate the *once defective, always defective-condition*.



Locations of partially-stuck pixel candidates.

Taking into account the size of the sensor $w \cdot h$, the simulation growth rates and amplitudes are:

$$\lambda_{ps} = \gamma \frac{n_2 - n_1}{(T_2 - T_1) \cdot (w \cdot h)}$$

$$\lambda_s = \gamma \frac{n_{s2} - n_{s1}}{(T_2 - T_1) \cdot (w \cdot h)}$$

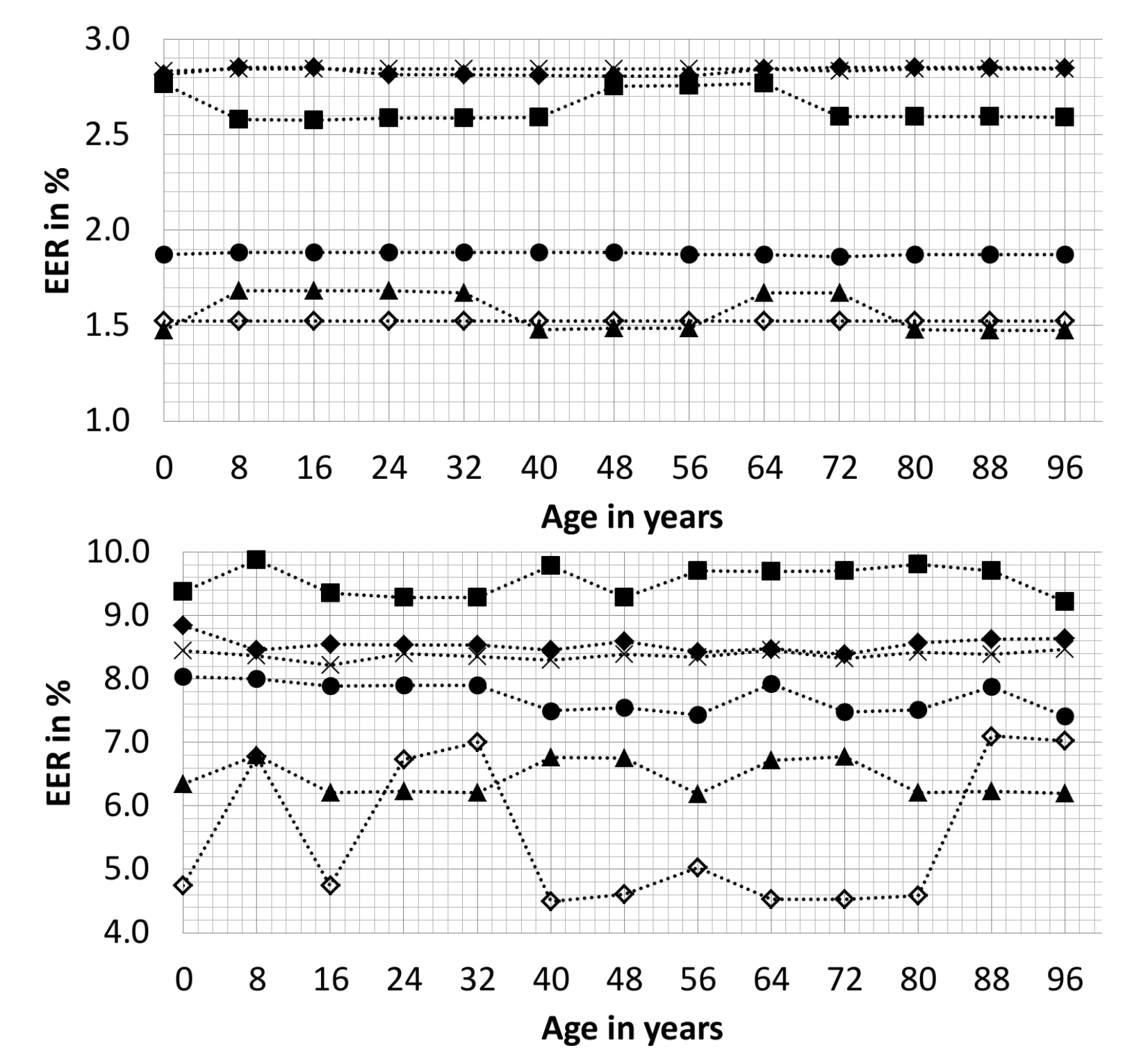
$$a_{ps} = \max(\hat{D}_{s_k})$$

$$a_s := 255$$

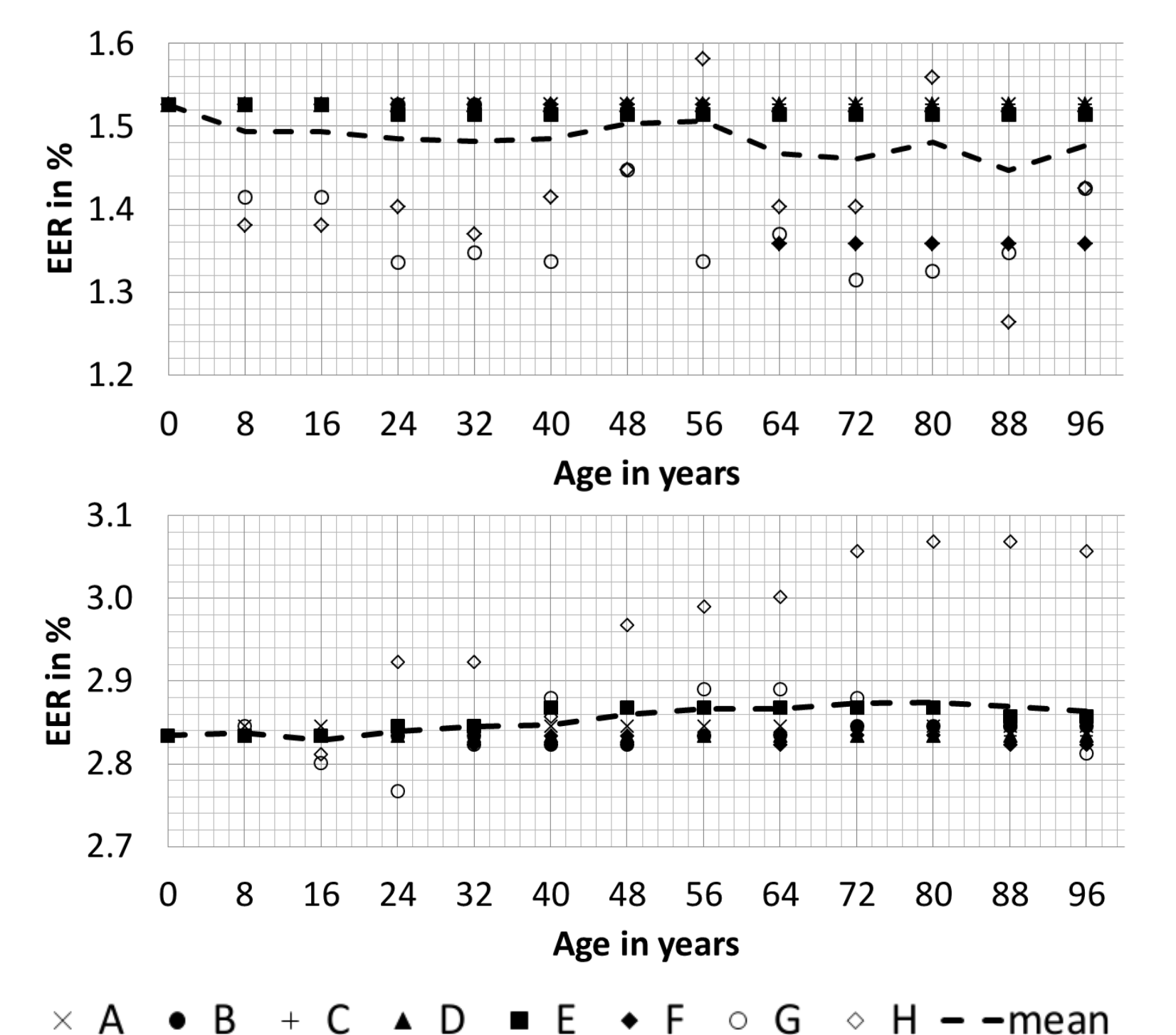
Simulated sensor ageing

For real sensors, pixel defects start to occur from a specific point in time T_0 with constant growth rate.

- **Poisson process** with λ_{ps} and λ_s
- Y_{T_0} might already contain pixel defects
- **Investigation of changes over a period of time** \rightarrow observed time frame does not matter



EER of six iris-signature algorithms. The segmentation was done by using CAHT (top) and WAHET (bottom) respectively.



EERs of the algorithms of Masek (top) and Ko *et al.* (bottom) with CAHT-segmentation for aged data sets.

Conclusion

- Sensor ageing influences the accuracy
- Sensitiveness to spiky noise (e.g. pixel defects)
- No trend observable
- System's accuracy depends on current physical condition of the sensor
- Texture ageing experiments based on evaluation of accuracy changes (e.g. the EER) are therefore **not entirely reliable**